

Two photoionization thresholds of N_3 produced by CIN_3 photodissociation at 248 nm: Further evidence for cyclic N_3

Peter C. Samartzis^{a)}

Department of Chemistry and Biochemistry, University of California Santa Barbara, Santa Barbara, California 93106

Jim Jr-Min Lin, Tao-Tsung Ching, Chanchal Chaudhuri, and Yuan T. Lee

Institute of Atomic and Molecular Sciences, Academia Sinica, P.O. Box 23-166, Taipei 106, Taiwan, Republic of China

Shih-Huang Lee

National Synchrotron Radiation Research Center, 101 Hsin-Ann Road, Science-Based Industrial Park, Hsinchu 30077, Taiwan, Republic of China

Alec M. Wodtke

Department of Chemistry and Biochemistry, University of California Santa Barbara, Santa Barbara, California 93106

(Received 6 June 2005; accepted 13 June 2005; published online 5 August 2005)

We present results of near-threshold photoionization of N_3 photofragments produced by laser photodissociation of CIN_3 at 248 nm. The time of flight of recoiling N_3 is used to resolve two photochemical channels producing N_3 , which exhibit different translational energy release. The two forms of N_3 resolved in this way exhibit different photoionization thresholds, consistent with their assignment to linear ($X^2\Pi_g$) and cyclic N_3 . This result agrees with the existing theoretical calculations of excited and ionic states of N_3 and strengthens previous experimental results which suggested that the CIN_3 photolysis produces a cyclic form of N_3 . © 2005 American Institute of Physics. [DOI: 10.1063/1.1993590]

There has been substantial interest in the photochemistry of CIN_3 (Ref. 1) due to its importance in chemical lasers,² yet only recently have we begun to understand its primary photochemical reaction dynamics. CIN_3 photodissociation proceeds by two distinct pathways. The first (“molecular”) pathway produces $NC1$ and N_2 and the second (“radical”) pathway produces $C1$ and N_3 . Photofragmentation translational spectroscopy (PTS) studies show that the radical channel is dominant ($95\% \pm 3\%$) over the molecular channel³ at one of the more commonly used photolysis wavelengths (248 nm). Using velocity map ion imaging⁴ (VMI) of $C1$ atoms to study the dominant radical channel, Hansen and Wodtke concluded that N_3 is produced with a bimodal internal energy distribution when CIN_3 is photolyzed at 235 nm,⁵ a behavior that was also later reported from PTS studies at 248 nm.³ Recently, more accurate thermochemical data⁶ along with high-level quantum-chemical computations^{7–9} helped to show that these observations are quantitatively consistent with the formation of N_3 in two isomeric forms: the $^2\Pi_g$ “linear azide” and the $^2B_1/{}^2A_2$ “cyclic N_3 .”⁵

Theory predicts the cyclic- N_3 electronic ground state to have three equivalent energy minima of 2B_1 symmetry separated by low-energy (0.0386 eV) transition states of 2A_2 symmetry allowing pseudorotation.^{7,8} At the 2B_1 minima, cyclic N_3 has the shape of an acute isosceles triangle with one short (double—1.235 Å) bond and two long (single—1.467 Å) bonds while at the 2A_2 transition states it becomes an obtuse

isosceles triangle with one long (1.5338 Å) and two short (1.3058 Å) bonds. The cyclic- N_3 isomer is predicted to lie 1.35 eV above linear azide and be frustrated by a large (1.5 eV) barrier to linearization.⁷ Furthermore the barrier to spin-allowed dissociation forming $N(^2D)+N_2$ is predicted to be larger than 1.4 eV. Quantum-chemical analysis of the doublet-quartet seam crossing reveals that cyclic N_3 is long lived with respect to dissociation to ground state products, $N(^4S)+N_2$ (Ref. 7), a prediction consistent with a recent report of bimodal translational energy distributions for N_3 observed by PTS.¹⁰ Calculations show that the geometric phase effect is large in cyclic N_3 .⁹

Ab initio calculations on N_3^+ predict an equilateral triangular structure for the $a'-{}^1A_1$ state with a N–N bond length of 1.3314 Å. Its energy was calculated to be 0.871 eV above the $N_3^+(X^3\Sigma_g^-)$ ground state.¹¹ These authors refer to peaks in the photoelectron spectra of N_3 ,¹² indicating states of N_3^+ that are 0.72 and 0.79 eV above the N_3^+ ground state to support their conclusions. Exploiting the literature value of the ionization energy of $N_3(X^2\Pi_g)$, 11.06 eV,¹² one predicts that the $a'-{}^1A_1$ state should lie 11.931 eV above the linear-azide or 10.58 eV above the cyclic- N_3 state. Recent *ab initio* calculations carried out at CCSD(T)/cc-pVTZ level of theory predict the cyclic N_3 adiabatic ionization energy to be $T_{ee} = 10.39$ eV (Ref. 13) (neglecting zero-point energy, ZPE). The ZPE (0.1644 eV) of the ground E -symmetry vibrational state of cyclic N_3 has been calculated carefully, including the geometric phase effect.⁹ The ZPE of cyclic N_3^+ (0.2421 eV) was calculated within the harmonic approximation.¹³ From

^{a)}Electronic mail: sama@chem.ucsb.edu

this, we arrive at a theoretically predicted ionization threshold, $T_{00}=10.47$ eV. It is reasonable to assume that if the *high-energy form* of N_3 produced by CIN_3 photodissociation at 248 nm possesses a cyclic structure, its ionization will lead to the $a'-^1A_1$ state of N_3^+ . If this is true, we expect to find the photoionization threshold for the excited form of N_3 close to the values predicted by theory.

The experiments discussed here were carried out at the Chemical Dynamics endstation of the 21A Beamline of the National Synchrotron Radiation Research Center in Hsinchu, Taiwan. We used synchrotron radiation to vary the photon energy used to ionize and detect N_3 fragments produced by CIN_3 laser photodissociation at 248 nm. By virtue of their differing translational energy releases, we are able to resolve the two forms of N_3 formed in the photodissociation and separately measure the photoionization thresholds for each. These results reveal a photoionization threshold for the energetic form of N_3 that is shifted to lower energy, consistent with the theoretically predicted energies described above. This provides additional evidence supporting the photochemical formation of cyclic N_3 .

A description of the apparatus has been previously published¹⁴ and only a brief description of the experiment will be given here. A mix of CIN_3 seeded in He carrier gas was prepared by passing a 10% Cl_2 mix in He over moist NaN_3 suspended in a cotton wool and then through a drying agent (Drierite) to remove excess water. The mix expanded supersonically through a solenoid valve (General Valve, Series 9) in the source chamber of the apparatus forming a molecular beam which was intersected at right angles, 54 mm downstream by the cylindrically focused output (2.25

$\times 8.5$ mm² spot size) of a KrF excimer laser (Lambda Physik LPX 210) operating at 248 nm. The photodissociation fragments were allowed to drift for another 100.5 mm through two separate differentially pumped chambers and were then intersected at right angles by synchrotron radiation (1.0 \times 1.0 mm² spot size) in a cryogenically cooled ultrahigh-vacuum ionization chamber.

The beamline radiation characteristics are available online.¹⁵ In these experiments, the photon energy spread of the fundamental synchrotron radiation in the 9.8–13-eV range is $\sim 3\%$ full width at half maximum (FWHM). Higher-order harmonics produced by the synchrotron undulator were filtered by appropriate noble gases. The photoions were focused by ion optics into a quadrupole mass filter and the m/z ratio of choice was detected by a Daly-type detector and counted by a multichannel scaler. The molecular beam is rotatable, allowing the measurement of time-of-flight (TOF) spectra at different laboratory angles Θ between the molecular beam and the detection axis. Initially we recorded the TOF spectra of $m/z=35$ (Cl^+) at a 13.3 eV synchrotron energy and of $m/z=42$ (N_3^+) in the 9.8–13 eV synchrotron energy range in 0.3 eV steps at $\Theta=20^\circ$, 40° , and 60° . Measurements for $m/z=42$ were repeated for $\Theta=20^\circ$, 45° , 50° , and 80° in steps as small as 0.04 eV in the 10.2–11.5 eV range to obtain a more accurate value for the ionization thresholds. Each TOF spectrum was averaged for $5\text{--}10 \times 10^4$ laser shots as needed to have adequate signal-to-noise ratio.

TOF spectra obtained in this fashion were fitted by the PHOTRAN forward-convolution program. This program simulates the time-of-flight spectrum based on center-of-mass

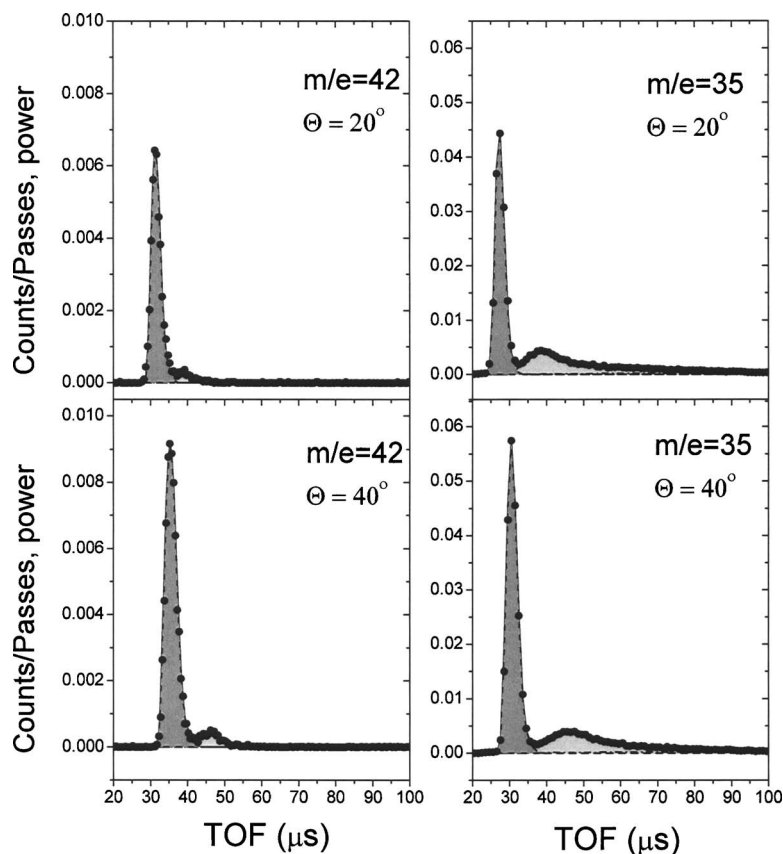


FIG. 1. Representative TOF spectra of $CIN_3 \rightarrow Cl + N_3$ photolysis at 248 nm. Fast and slow channels have been previously attributed to formation of electronic-ground-state linear azide and a high-energy form of N_3 consistent with “cyclic” N_3 , respectively. As the high-energy form of N_3 appears with lower translational energy release than that of linear azide, the two channels can be resolved in these TOF spectra. The momentum-matched Cl photofragment must and does exhibit a similar bimodal character. The Cl^+ TOF spectra shown here employed 13.3 eV photons for the photoionization of Cl . The N_3^+ TOF spectra shown here employed 10.7-eV photons for photoionization. Experimental data are represented as filled circles, slow and fast N_3 channel fits as dotted and dashed lines, respectively, and the total fit as continuous line. The Y axis shows ion counts per laser shot, normalized to the laser power.

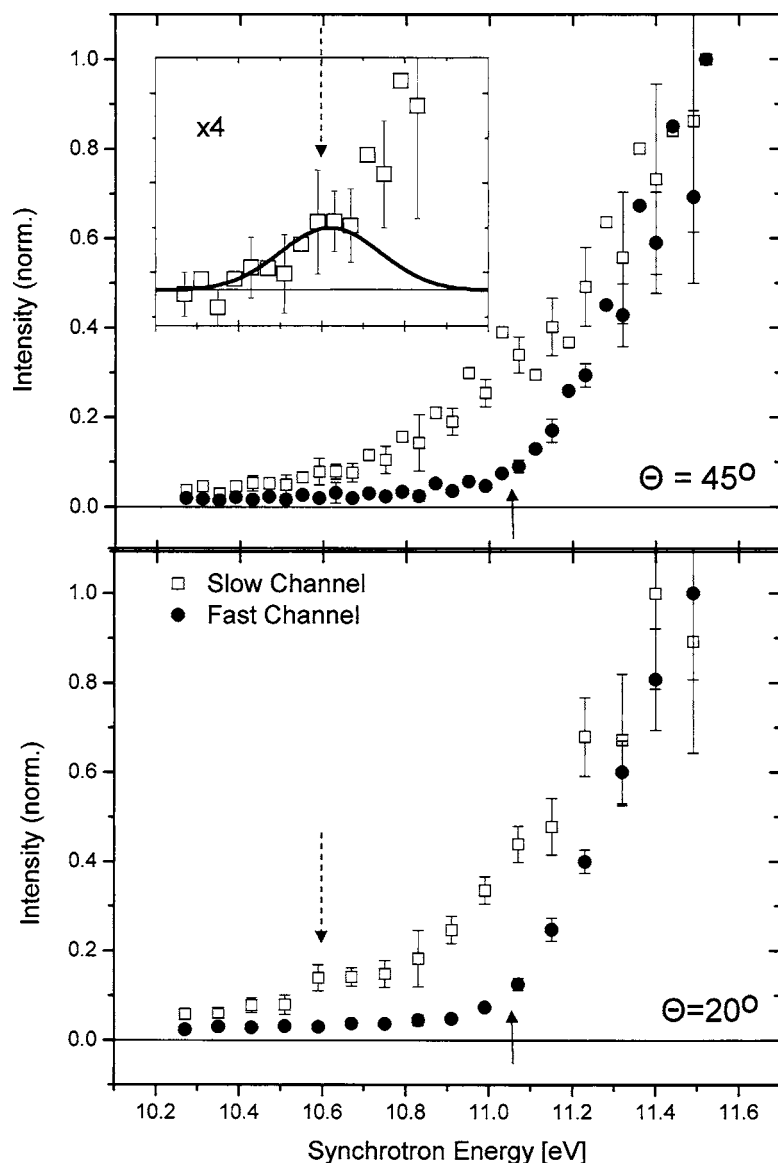


FIG. 2. Photoionization of the two TOF-resolved forms of N_3 vs ionization photon energy. Normalized integrated intensities for the slow (open rectangles) and fast (filled circles) channels at laboratory angles of $\Theta=20^\circ$ (lower panel) and $\Theta=45^\circ$ (upper panel). The inset in the upper panel shows the 45° data on an expanded scale. A Gaussian function centered at 10.62 eV represents the energy spread of the synchrotron radiation. The solid arrows indicate the literature value for the ionization threshold of linear N_3 and the dashed arrows the expected value for cyclic N_3 . Statistical error bars were calculated at 90% confidence for the 45° data points where more than two measurements were available using the *student's t-test*. The error bars shown for 20° are estimated based on comparison with the 45° data.

translational energy distributions $P(E)$ which are iteratively adjusted until a satisfactory fit to the data is obtained. Beam velocity, laboratory angle, dissociation and ionization intersection sizes, finite angular acceptance angle of the detector, laser power, and polarization are additional program parameters.

Representative fitted TOF spectra for $m/z=35$ (Cl^+) and $m/z=42$ (N_3^+) are presented in Fig. 1 for two laboratory angles Θ . All TOF distributions are bimodal, exhibiting a “fast” and a “slow” component. The fast Cl^+ peak corresponds to production of ground linear azide; the slow peak corresponds to formation of the high-energy form of N_3 , consistent with cyclic N_3 .⁵ The ratio of the integrated areas of the two components is about 4:1, consistent with previous experimental measurements. For $m/z=42$ (N_3^+), the slow peak is also clearly visible, however, the ratio between the fast and slow components changes with photoionization wavelength, indicating that the two forms of N_3 have different photoionization properties.

Fitting data like that of Fig. 1 allows us to determine the relative contributions of the fast and slow channels at many

photoionization wavelengths. The integrated intensity of each channel is shown as a function of ionizing photon energy in Fig. 2 for laboratory angles of $\Theta=45^\circ$ (top panel) and 20° (bottom panel). In each plot, the filled circle points belong to the fast channel and the open rectangles to the slow channel. Intensities were normalized to the maximum of the respective channel at 11.5-eV synchrotron energy.

Both channels exhibit an abrupt increase in intensity between 10.2 and 11.2 eV. For the fast channel, the observed threshold agrees well with the previously determined photoionization threshold for linear azide (11.06 eV), indicated in Fig. 2 by the solid arrows. The slow channel clearly exhibits a lower photoionization threshold, around 10.6 eV, which is close to the theoretically derived value for ionization of cyclic N_3 producing $a'^{-1}A_1 N_3^+$ (indicated in Fig. 2 by the dashed arrows).

We note that at all laboratory angles, ion signal is present well below the respective ionization threshold energies. Synchrotron radiation produced from an undulator exhibits higher harmonics. Thus, light that is nominally of a photon energy of 10.2 eV has other photon energies present (20.4

eV, 40.8 eV, ...). Nearly all of this light is removed by the gas filter; however, the filtering is not effective for photons in the transparent window of the gas. This effect increases the background in the measurement but does not change the difference in the ionization thresholds for the two forms of N_3 .

In conclusion, we observe two photoionization threshold energies for the two forms of N_3 that are formed in CIN_3 photolysis at 248 nm. The observed thresholds are consistent with assignments of the two forms of N_3 to (1) electronic ground-state linearazide and (2) cyclic N_3 . This result suggests that the ionization of cyclic N_3 leads to the $a'^{-1}A_1$ ion state.

ACKNOWLEDGMENTS

This work was in part supported by a grant from the Air Force Office of Scientific Research (Grant No. FA9550-04-1-0057). One of the authors (P.C.S.) would like to thank the Institute of Atomic and Molecular Sciences, Academia Sinica, Taipei, Taiwan for financial support and the National Synchrotron Radiation Research Center personnel for their help in conducting those experiments.

- ¹R. D. Coombe, D. Patel, A. T. Pritt, and F. J. Wodarczyk, *J. Chem. Phys.* **75**, 2177 (1981); R. D. Coombe, J. V. Gilbert, S. S. Beaton, and N. Mateljevic, *J. Phys. Chem. A* **106**, 8422 (2002); A. V. Komissarov, G. C. Manke, S. J. Davis, and M. C. Heaven, *ibid.* **106**, 8427 (2002).
- ²G. C. Manke and G. D. Hager, *J. Mod. Opt.* **49**, 465 (2002).
- ³A. M. Wodtke, N. Hansen, J. C. Robinson, N. E. Sveum, S. J. Goncher, and D. M. Neumark, *Chem. Phys. Lett.* **391**, 334 (2004).
- ⁴A. J. R. Heck and D. W. Chandler, *Annu. Rev. Phys. Chem.* **46**, 335 (1995); A. Eppink and D. H. Parker, *Rev. Sci. Instrum.* **68**, 3477 (1997).
- ⁵N. Hansen and A. M. Wodtke, *J. Phys. Chem. A* **107**, 10608 (2003).
- ⁶N. Hansen, A. M. Wodtke, A. V. Komissarov, and M. C. Heaven, *Chem. Phys. Lett.* **368**, 568 (2003); N. Hansen, A. M. Wodtke, A. V. Komissarov, K. Morokuma, and M. C. Heaven, *J. Chem. Phys.* **118**, 10485 (2003).
- ⁷P. Zhang, K. Morokuma, and A. M. Wodtke, *J. Chem. Phys.* **122**, 014106 (2005).
- ⁸M. Bittererova, H. Ostmark, and T. Brinck, *J. Chem. Phys.* **116**, 9740 (2002); D. Babikov, P. Zhang, and K. Morokuma, *ibid.* **121**, 6743 (2004).
- ⁹D. Babikov, B. Kendrick, P. Zhang, and K. Morokuma, *J. Chem. Phys.* **122**, 044315 (2005).
- ¹⁰N. Hansen, A. M. Wodtke, S. J. Goncher, J. Robinson, N. Sveum, and D. M. Neumark, *J. Chem. Phys.* (to be published).
- ¹¹R. Tarroni and P. Tosi, *Chem. Phys. Lett.* **389**, 274 (2004).
- ¹²J. M. Dyke, N. B. H. Jonathan, A. E. Lewis, and A. Morris, *Mol. Phys.* **47**, 1231 (1982).
- ¹³V. Mozhayskiy and A. I. Krylov (private communication).
- ¹⁴J. J. Lin, Y. Chen, Y. Y. Lee, Y. T. Lee, and X. M. Yang, *Chem. Phys. Lett.* **361**, 374 (2002).
- ¹⁵<http://srccbl.nsrc.org.tw/servlet/blDocReader?param=21A>